EARTHQUAKE DAMAGES AND REMEDIAL WORKS FOR AN EARTH DAM WITH ASPHALT FACING

Y. Nakamura[1], Y. Ohne[2], K. Narita[2], T. Okumura[2]
K. Nomura[3], M. Shimazaki[4] and T. Mizuno[5]

INTRODUCTION

Higashi-fuji dam is an earth dam of about 25m in height which was constructed in 1971 for irrigation purpose at the foot of Mt. Fuji. The embankment was principally constructed of volcanic sand, Scoria, which was supplied by cutting the original ground on the opposite side of the embankment, as shown in Fig.1. Because the cut ground was highly permeable, the reservoir foundation as well as the embankment slope was covered by asphalt pavement. The standard cross section of the embankment is illustrated in Fig.2. Details of structure of the pavement on the slope and the foundation are presented in circles (a) and (b), respectively.

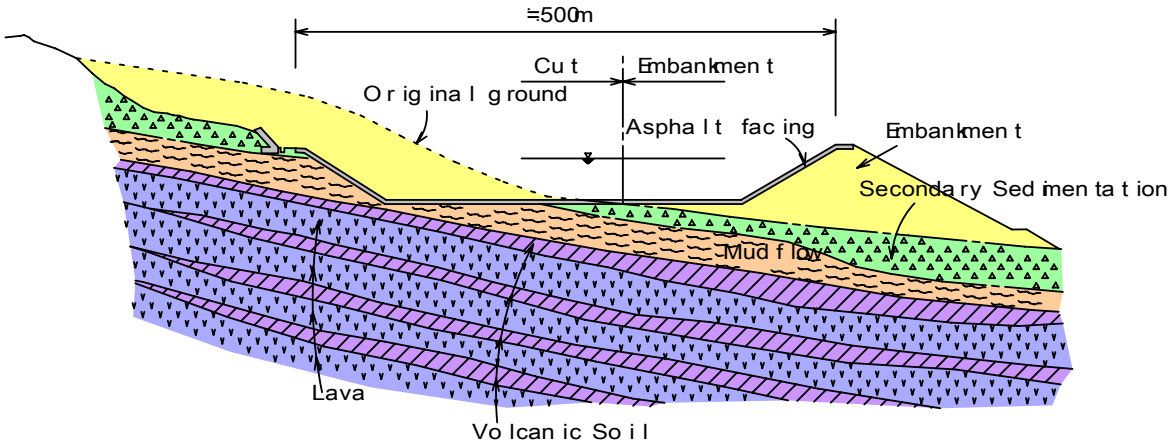

Fig.1 Cross Section of Higashi-fuji Dam

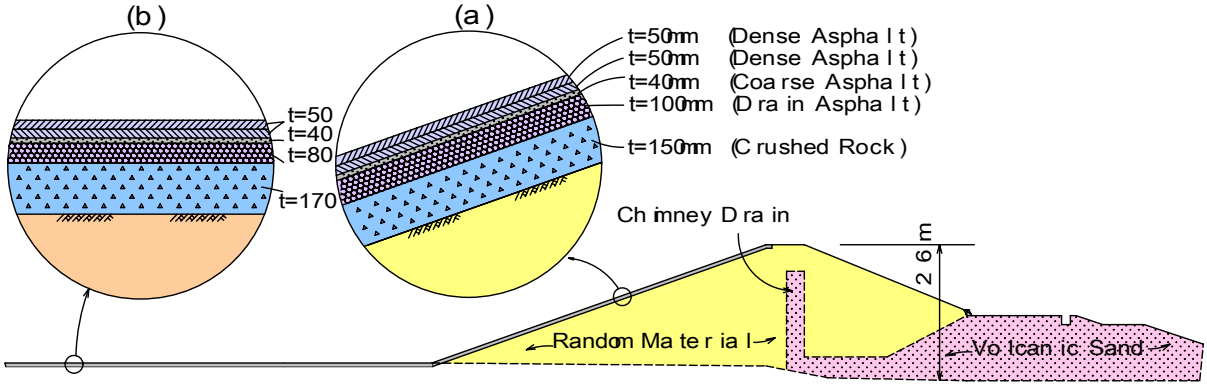

Fig.2 Standard Cross Section of Embankment and Structure of Facing

On March 6 in 1996, the dam was attacked by the Yamanashi-Tobu earthquake of magnitude 5.8 with the epicenter about 15km north from the dam, and suffered severe damages of cracking on the surface of the asphalt pavement, as shown in Fig.3. The records of the maximum acceleration showed α_B=85gals at the base foundation and α_t=380gals at the crest of the embankment, respectively.

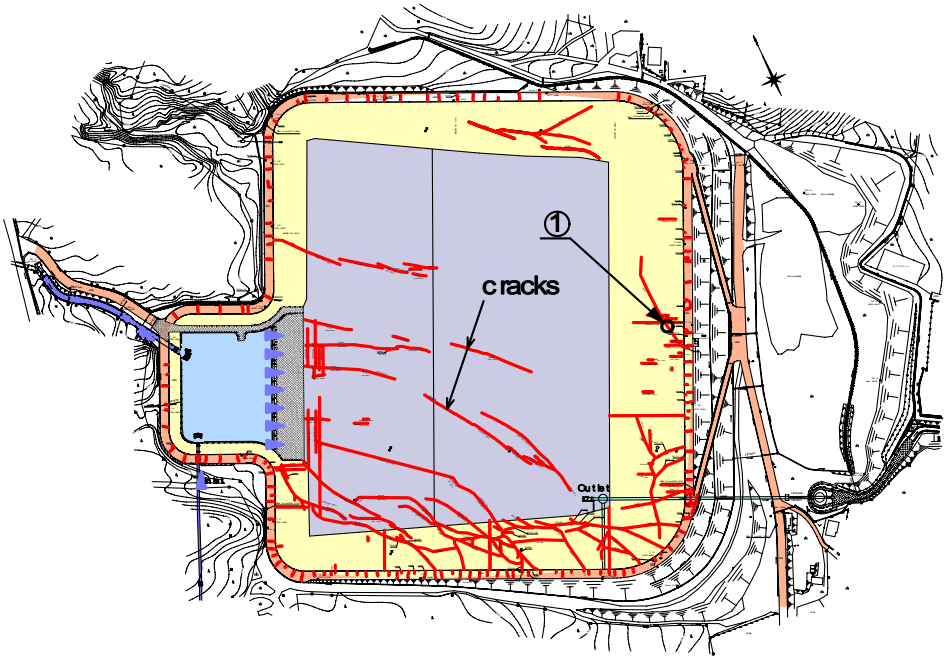

Fig.3 Plan View of Reservoir

DAMAGE INVESTIGATION

A close investigation of damages was made after lowering the reservoir level completely to the bottom from about 2/3 of the full height. As a result, damages were not found in the body of the embankment. Severe cracking damages were detected to a large extent in the asphalt pavement covering the embankment slope and the reservoir foundation, as shown in Fig.3. As is seen in Photo-1, cracks have the maximum width of 10mm and on the whole open to the depth of the pavement.

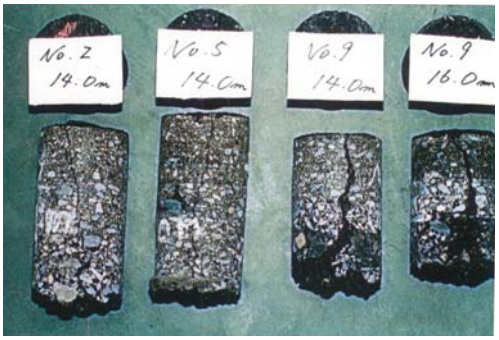

Photo-1 Cracks in Asphalt Facing
(taken at ① in Fig.3)

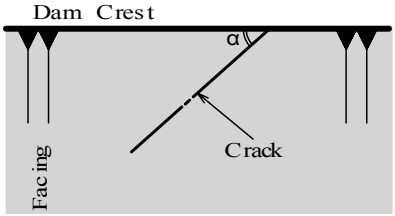

(a) Asphalt Facing

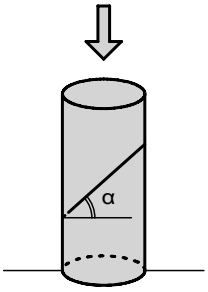

(b) Compression test

Fig.4 Direction of Cracking

Most of cracks detected in the field run to the direction from 35 to 80degrees, average about 64degrees, against the axis of the dam. This angle resembles to the direction of shear cracks which appear in the unconfined compression test, as illustrated in Fig.4. As one of possibilities, therefore, it is considered that the asphalt facing on the slope was subjected to cyclic compression and tension stresses in the direction along the slope, and shear cracks developed diagonally to the dam axis.

DYNAMIC RESPONSE ANALYSIS OF EMBANKMENT

Analytical Procedure

Input Seismic Wave: Because the earthquake records obtained at Higashi-fuji dam site consisted only of the maximum value of acceleration, without their time histories, another seismic records observed at Miho dam (JCOLD, 2002), which is a central core type rock-fill dam of 95m in height and located about 13km from the epicenter, were used for assuming the input motion of acceleration in the analysis, as follows.

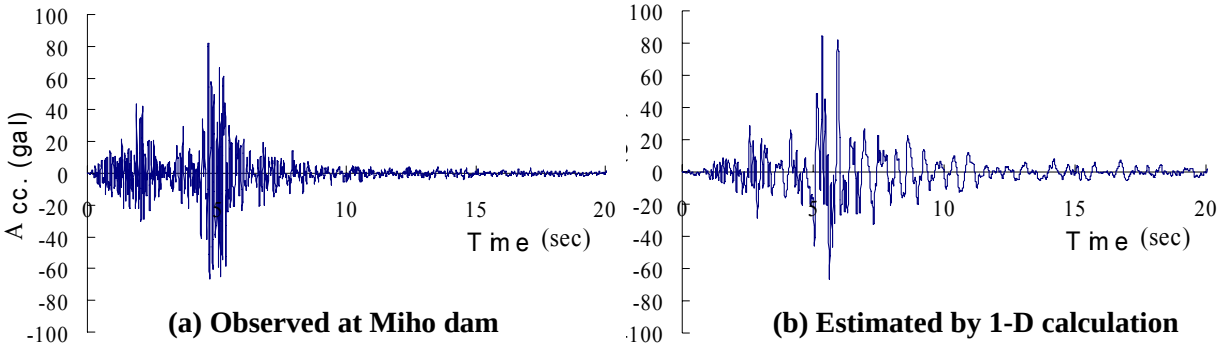

(a) Observed at Miho dam **(b) Estimated by 1-D calculation**

Fig.5 Observed and Estimated Earthquake Motion

Higashi-fuji dam rests on a soil foundation, sedimentation of mud flow, while the foundation of Miho dam is composed principally of tuff breccia. The input motion was therefore made by applying the multiple reflection theory (Schnabel et al., 1972) on a 1-D simulation model of the base foundation of Higashi-fuji dam, where the base foundation of mud flow of 600m thick, which covers the andesite base rock, can be represented by three soil layers having different dynamic properties. By using the values of the modulus of rigidity *G* determined from the results of elastic wave exploration survey, an earthquake motion was evaluated as shown in Fig.5(b), which is compared with the original wave of Miho dam in Fig.5(a). Fourier spectra of both waves are compared in Fig.6. It is recognized in the figure that longer period of motion is dominant in the estimated wave, and that the predominant frequency ranges from 1 to 2Hz, in contrast to the observed wave of 8 to 10Hz.

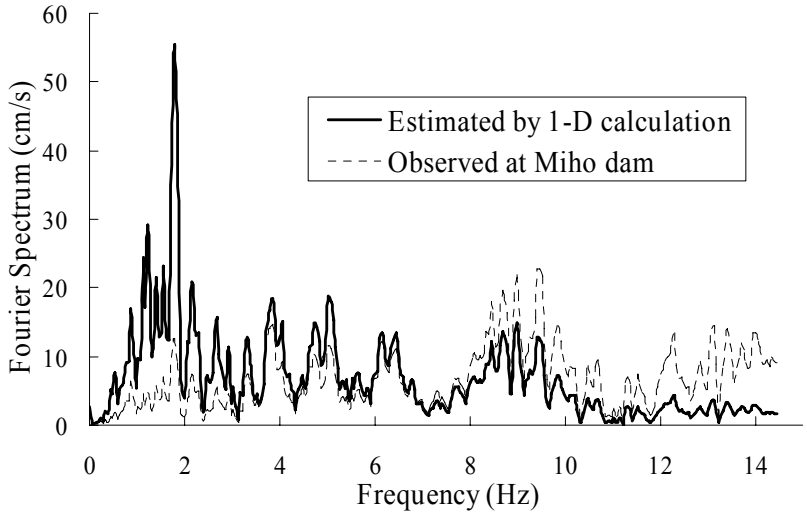

Fig.6 Fourier Spectrum of Observed and Estimated Earthquake Motion

Dynamic Deformation Properties: Field investigation of 13 core borings carried out in Higashi-fuji dam after the earthquake reveals that the embankment was really sound without any damages. Laboratory tests were conducted for fill materials obtained in the boring. Cyclic tri-axial tests were also done for volcanic sand on specimens of ϕ 50mm×H100mm under CU condition. Analytical procedure employed in this paper is the equivalent linear method (Idriss et al., 1973), and the Hardin-Drnevich model of Eq.(1) is used to express the dynamic deformation properties of fill materials, as follows:

$$G/G_0 = \frac{1}{1+(\gamma/\gamma_r)} \qquad h = h_0 \frac{\gamma/\gamma_r}{1+(\gamma/\gamma_r)} + h_d \qquad (1)$$

where G and h are the shear modulus and the damping factor at shear strain γ, G_0 and h_0 are those at small strain, γ_r is the reference strain, and h_d is the radiation damping, respectively.

Table-1 Dynamic Properties of Fill Material

	Shear Modulus	Damping Ratio	Reference strain
Random material	G_0=40.0×(σ_m'/p_a)$^{0.47}$	h/h_0=0.14	γ_r = 4.8×10^{-3}×(σ_m'/p_a)$^{0.75}$
Volcanic Sand	G_0=47.5×(σ_m'/p_a)$^{0.76}$	h/h_0=0.12	γ_r = 9.4×10^{-4}×(σ_m'/p_a)$^{0.60}$

p_a: atmospheric pressure

The parameters γ_r, G_0 and h_0 in Eq.(1) are determined in the calculation as noted in Table-1, where parameters of the volcanic sand were derived as above and those of the random fill were estimated from test results on similar fill materials (Ohne, 1983). Concerning G_0-value

of the random fill, $G_0=40(\sigma_m'/p_a)^{0.47}$ in Table-1 was adopted through trial calculation, by changing G_0 in the range $G_0=(35\sim 50)(\sigma_m'/p_a)^{0.47}$ to have a similar magnification factor of $\alpha_t/\alpha_B \fallingdotseq 4.5$ as observed in the field. As for damping properties, the radiation damping h_d in Eq.(1) was taken into account in the analysis, in addition to the material damping, and the value of $h_d=0.1$ was evaluated by use of Kanai-equation (Sezawa, 1963) for the ratio of velocity impedance between the embankment and the foundation.

Cases of Calculation: Response analysis was made for the following two cases. One is the case of the input acceleration of $\alpha_B=85$gals, to reproduce dynamic behavior of the dam and to discuss mechanism and causes of cracking appeared in the asphalt facing. The other is the case of $\alpha_B=200$gals, to evaluate damages of the embankment when it is subjected to a strong earthquake equivalent to the design value of acceleration, and to study appropriate stiffness and ductility of asphalt mixture to be required for use in remedial works.

Results of Analysis

Predominant Frequency: The first natural frequencies of the embankment calculated in the response analysis showed 1.91Hz for $\alpha_B=85$gals and 1.64Hz for $\alpha_B=200$gals which are in the range from 1 to 2Hz and rather close to the predominant frequency of the input seismic wave. It is therefore inferred that the response behavior of the embankment during the earthquake is in a state of the first mode of vibration and close to a resonant state, which results to have a considerably high value of acceleration response like as $\alpha_t/\alpha_B \fallingdotseq 4.5$ observed in the field.

Yield Acceleration: In the stability analysis of slopes based on the seismic coefficient method, the mean value of acceleration of soil mass above a circular sliding plane by which the value of safety factor becomes to unity is defined as the yield acceleration (Makdisi and Seed, 1977), and permanent displacement can be evaluated along the sliding plane by integrating excess of acceleration over the yield value (Newmark, 1960). Stability analysis of Higashi-fuji dam was made by taking the mean value of strength parameters (c, ϕ) for the design seismic coefficient of $k_h=0.2$. Critical sliding planes were obtained as No.1 on the upstream side and as No.6 on the downstream side as shown in Fig.7. The values of the yield acceleration obtained from slope stability analysis and the maximum mean horizontal acceleration from dynamic response analysis are compared in Table-2 for every 9 sliding planes in Fig.7. It is noted that even in the case of $\alpha_B=200$gals the maximum mean acceleration of sliding soil mass is small enough as compared with the yield acceleration and that sufficient safety must be maintained

against sliding failure.

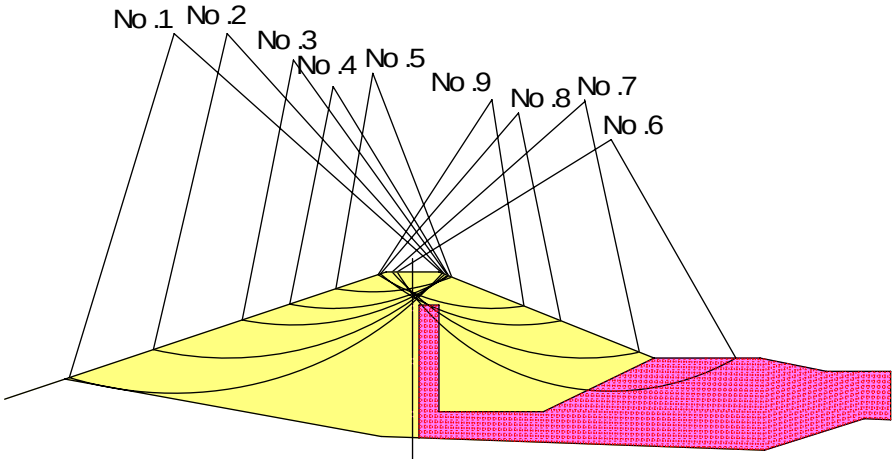

Fig.7 Circular Slip Surfaces

Table-2 Yield and Maximum Mean Acceleration for circular sliding

No. of Slip Circle	Yield Acc.(gals)	Max. Mean Acc.(gals)	
		α_B=85gals	α_B=200gals
No.1	323	116	202
No.2	382	148	251
No.3	500	212	380
No.4	627	264	468
No.5	882	353	658
No.6	304	171	300
No.7	372	186	369
No.8	485	212	480
No.9	608	239	571

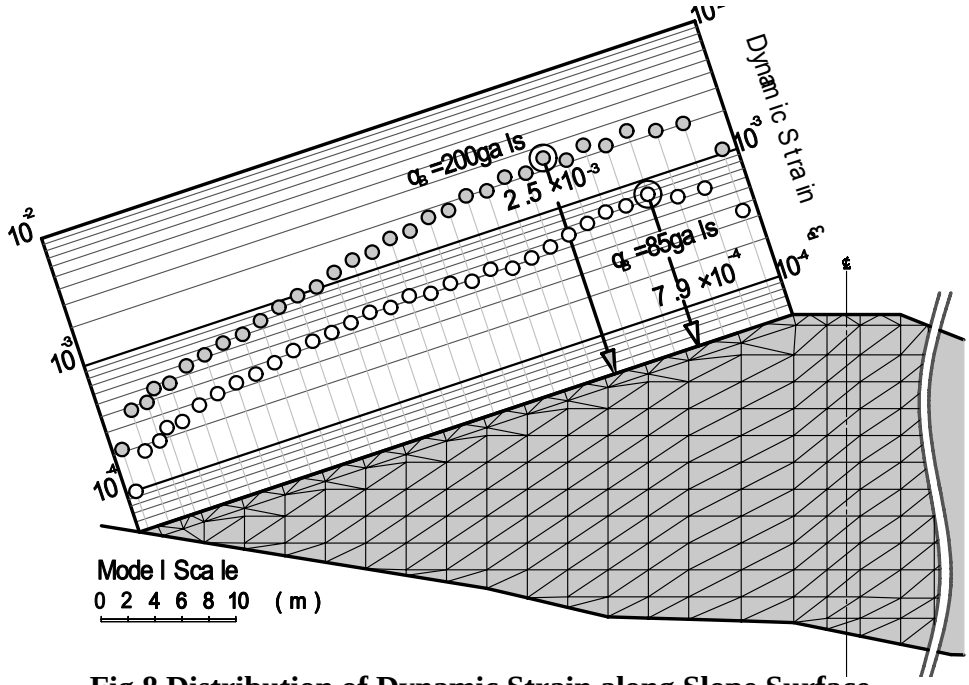

Fig.8 Distribution of Dynamic Strain along Slope Surface

Strain Distribution: The asphalt facing should be subjected to cyclic action of compression and tension forces along the slope when the facing vibrates in harmony with the embankment. Dynamic strain developed in the facing is evaluated here for every section of adjacent two nodal points, as a ratio of the difference of displacements along the slope to the distance between the points. Distributions of the maximum values of the dynamic strain ε_d are drawn for every element along the slope, as shown in Fig.8. It is seen that the dynamic strain ε_d takes its maximum value at around the mid-height of the slope, being $\varepsilon_{dmax}=7.9\times10^{-4}$ for α_B=85gals, and $\varepsilon_{dmax}=2.5\times10^{-4}$ for α_B=200gals.

DYNAMIC PROPERTIES OF ASPHALT MIXTURE

Test Apparatus and Procedures

Series of cyclic loading tests were conducted on the asphalt mixtures used for the facing, in order to investigate such fundamental mechanical properties as dynamic stress-strain behavior, time dependency of deformation and cracking potential. The specimen is prepared in the shape of dumbbell as shown in Photo-2 to avoid stress concentration at the loading ends. Samples measured and adjusted to have standard density are uniformly laid in 2 layers, and compacted with a small tamper. The specimen is attached at both ends to a fixed frame by using sulfur mortar, and is cured in 24 hours under the temperature of 0°C in a curing tank. The test apparatus is shown in Photo-3, where cyclic loading is controlled by an electro hydraulic servo system and a specimen is loaded in the vertical direction by sine wave.

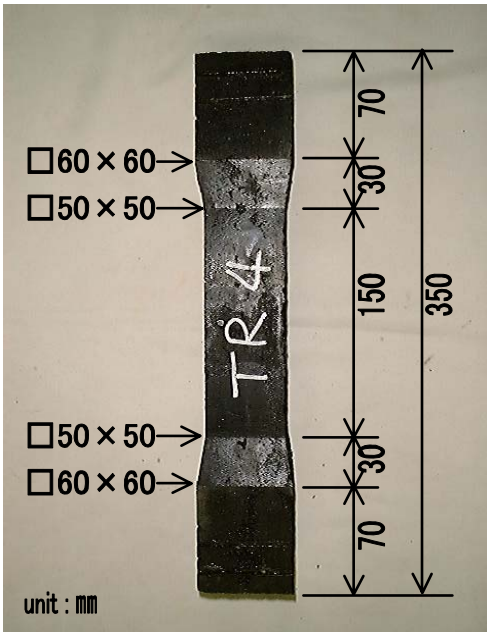

Photo-2 Shape of Specimen

Photo-3 Test Apparatus

Materials and Test Conditions

In this series of mechanical tests, two different types of asphalt (binder) are compared; straight asphalt (60/80) which is used as a usual binder of the asphalt mixture and the Super-Flexphalt developed for the purpose of improving deformation performance under a low temperature. The blending of the mixtures is the same for these binders. The cyclic loading tests are done by strain control in sine wave, by changing the loading rate of frequency in three different levels as 1Hz, 2Hz and 4Hz under a constant temperature of 0°C indicated at the time of the earthquake.

Test Results and Discussions

Dynamic Deformation Parameters: From the measurement of the axial load P and the axial displacement d of a specimen, the axial stress and strain (σ, ε), shear stress and strain (τ, γ), Young's modulus E, and the modulus of rigidity G are determined, respectively, in the followings, where A and H are the sectional area and the height of the specimen, and Poisson's ratio ν is assumed to be 0.5 in the calculation.

$$\sigma = \frac{P}{A}, \quad \tau = \frac{\sigma}{2}, \quad \varepsilon = \frac{d}{H}, \quad \gamma = (1+\nu)\varepsilon, \quad E = \frac{\sigma}{\varepsilon}, \quad G = \frac{\tau}{\gamma} = \frac{E}{2(1+\nu)} \qquad (2)$$

Characteristics of Skeleton Curves: Fig.9 shows $\tau \sim \gamma$ hysteresis loop and skeleton curve of the two mixtures at the condition of temperature of 0°C and frequency of 1Hz; both $\tau \sim \gamma$ loop and skeleton curve are drawn by solid line for the straight asphalt mixture and by broken line for the Super-Flexphalt mixture. The skeleton curve is composed of successive points of stress and strain amplitude of cyclic loading. The skeleton curve of the straight asphalt mixture shows linearly elastic behavior having a high modulus of elasticity like a brittle material, and that of the Super-Flexphalt mixture much more large plastic deformation over the yield point to failure like a ductile material.

Characteristics of Fatigue Failure: Fig.10 shows the relationship between the amplitude of axial strain ε in the test and the number of cycles N_f to cause failure. It is seen that the value of the dynamic strain ε decreases with the increase in frequency f of loading, and that the Super-Flexphalt mixture can be highly flexible, having 6 to 9 times higher value of ε as compared to the straight asphalt one. The relation curves of $\varepsilon \sim N_f$ in Fig.10 correspond to fatigue failure and can be approximated by a simple formula as $\varepsilon = A \times N_f^{\,B}$. The coefficient A and B of the formula have some relations with the loading frequency f, and are expressed in this series of tests as shown in Fig.11.

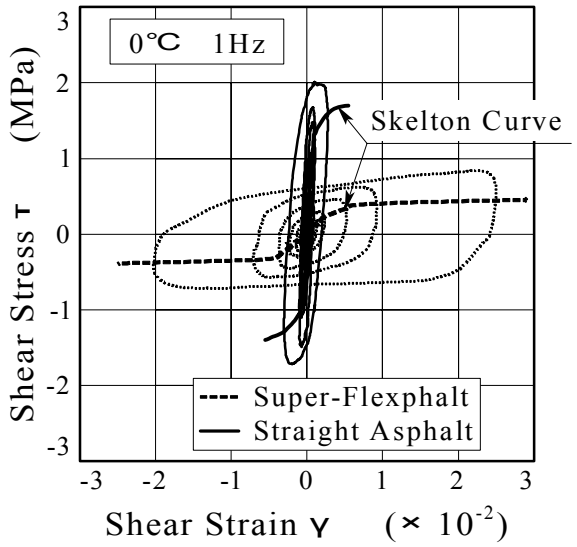

Fig.9 $\tau \sim \gamma$ Relation and Skeleton Curve

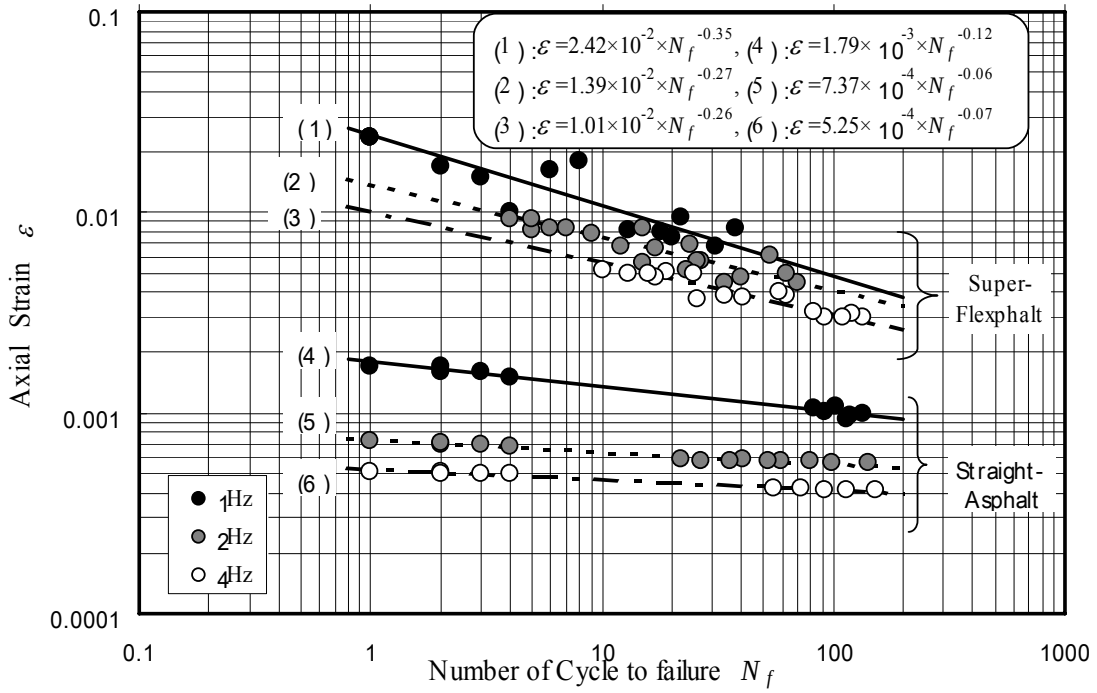

Fig-10 $\varepsilon \sim N_f$ Relation

EVALUATION OF EARTHQUAKE DAMAGES OF ASPHALT FACING

Concept of Accumulated Damage: Fig.12(a) shows a time history of dynamic strain ε_d developed along the embankment slope, at the point where the strain has its maximum value of $\varepsilon_{dmax}=7.9\times10^{-4}$, in the case of α_B=85gals. Let us consider in this figure a time difference Δt_i from a zero-crossing point of ε_d to the next zero-crossing point as a half cycle of vibration, and the peak value of ε_d during this Δt_i as its strain amplitude $\Delta\varepsilon$. Regarding each half cycle

as a part of harmonic wave of the amplitude $\Delta\varepsilon$, an equivalent frequency can be defined as $f_{ev}=1/(2\Delta t_i)$. The concept of accumulated damage is now introduced to evaluate earthquake cracking damages of the asphalt facing of Higashi-fuji dam. By using the relationship between frequency f and the coefficients A, B in Fig.11, and that between the dynamic strain ε and the number of cycles N_f to cause failure in Fig.10, the value of N_{fi} which corresponds to a half cycle of vibration of $(f_{ev}, \Delta\varepsilon)_i$ is obtained. The damage index is then defined by $\Delta D_i=1/(2N_{fi})$ for each half cycle, and is accumulated for a series of vibration as $D=\Sigma\Delta D_i$ to evaluate earthquake damages of the asphalt facing.

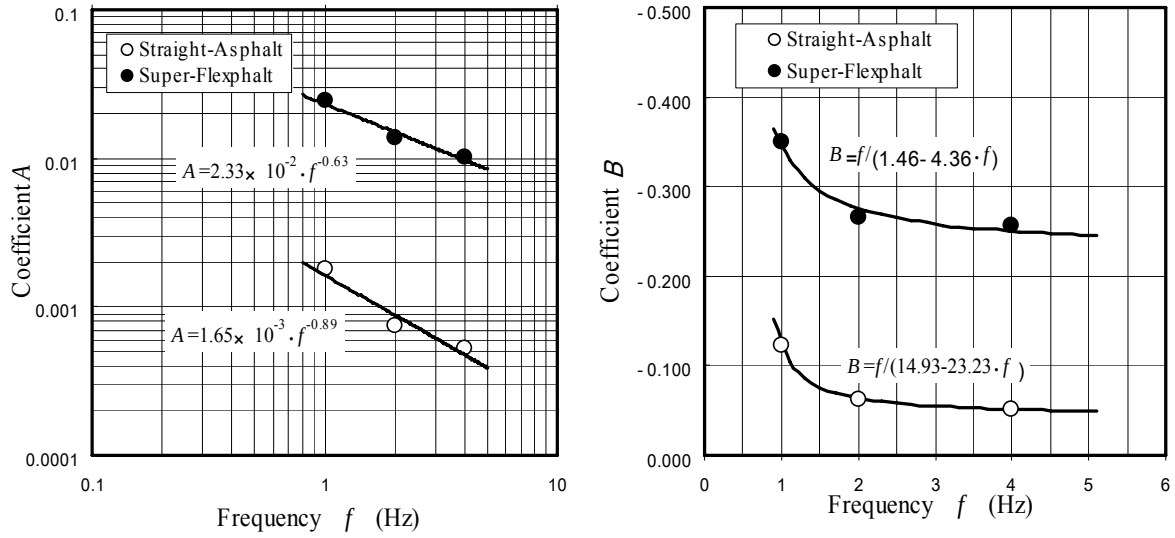

Fig-11 Coefficients *A*, *B* and Frequency

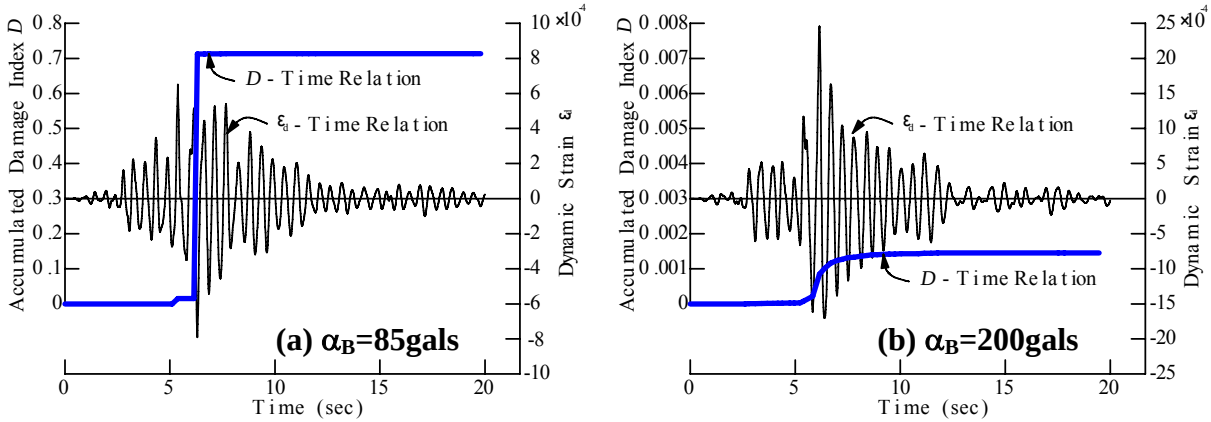

Fig. 12 Time Histories of *D* and ε_d

Damage Calculation: Variation of the accumulated damage index D with time is calculated in Fig.12(a) by applying experimental results of the straight asphalt mixture, and the ultimate value of D is obtained as 0.71. Although fatigue failure of steel structure is normally judged in

the range of $D > 1.0$, cracking damages observed in the dam is properly understood even in case of $D \fallingdotseq 0.7$ because more than 30years have passed since the asphalt facing was constructed and aging is considered to be another influential factor to cause failure. Another set of calculation for the Super-Flexphalt and α_B=200gals is shown in Fig.12(b), taking considerably small value of D=0.003. The maximum value of dynamic strain becomes to be $\varepsilon_{dmax}=2.5\times10^{-3}$ in this case, much more exceeding flexibility of the straight asphalt mixture.

REMEDIAL WORKS FOR THE ASPHALT FACING

Remedial works for the asphalt facing were done by overlaying watertight asphalt concrete of Super-Flexphalt after cutting and removing the damaged part of the pavement. Several laboratory tests were conducted beforehand on the repair materials to make sure of their stability during construction and weather resistance. As for the former, the slope flow test, which is usually done to investigate resistance against plastic flow in high temperature range, was done for a slope of inclination 1:2.5 (about 22degrees) and setting test temperature as 60degrees by assuming a temperature of the surface of pavement during summer. The test results are listed in Table-3. It is readily recognized that the flow value of the asphalt mixture of the Super-Flexphalt becomes to be about one-third of that of the straight asphalt (60/80) mixture, showing its higher resistance against plastic flow.

Table-3 Flow Values in Slope Flow Test (1/100mm)

Asphalt	after 24 hours	after 48 hours
Super-Flexphalt	68	68
Straight Asphalt	191	191

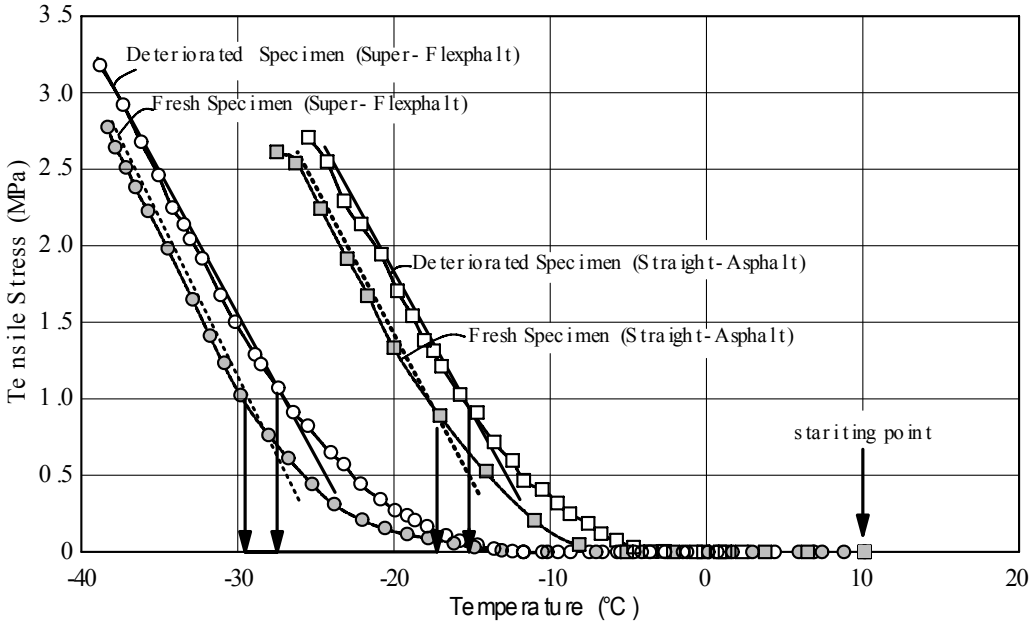

Fig. 13 Low Temperature Cracking Tests after Deterioration

In order to investigate the weather resistance, cracking tests were carried out under a low temperature on samples deteriorated in advance. Deterioration was realized by applying PAV (Pressure Aging Vessel), one of the US/SHRP testing methods, where each asphalt mixture was deteriorated by supplying oxygen and heat. In low temperature cracking tests, limit temperature of stress relaxation is evaluated by examining increasing rate of tensile stress developed in a specimen when it is restrained in both ends and its temperature is decreased in a constant rate. Test results are presented in Fig.13, indicating that the asphalt mixture of Super-Flexphalt has considerably high capacity of stress relaxation after deteriorated as compared with that of straight asphalt (60/80) usually used for watertight asphalt concrete.

SUMMARIES

Causes of earthquake damages of an asphalt facing are classified in two categories; one is a cause due to cyclic action of stresses along the facing and the other is due to permanent displacement accompanied by a sliding of embankment body. Damage evaluation on the basis of yield acceleration and permanent displacement of a sliding soil mass is not satisfactory in the present case, while the concept of accumulated damage index is considered to be a powerful measure to evaluate cracking potential in the asphalt facing.

REFERENCES

Idriss, I.M., Lysmer, R.H. and Seed, H.B., QUARD-4, a computer program for evaluating the seismic response of soil structure by variable damping finite element procedures, *EERC Report No.73-16*, 1973.

JCOLD, Acceleration records on dams and foundations No.2, 2002.

Makdisi, F.I. and Seed, H.B., A simplified procedure for estimating earthquake induced deformation in dams and embankments, *UBC/EERC-77/9*, 1977.

Newmark, N.M., Effects of earthquakes on dams and embankments, *Geotechnique, 15, No.2*, 139-160, 1960.

Ohne, Y. et al., Fundamental study on earthquake resistant design of fill-type dam, *Proc. of J SCE*, 1983.

Schnabel, P.B., Lysmer, J. and Seed, H.B., Shake- a computer program for earthquake response analysis of horizontally layered sites, *EERC 77-12*, 1972.

Sezawa, K. and Kanai, K., Damping in seismic vibrations of a surface layer due to an obliquely incident disturbance, *Earthquake Research Institute No.14*, 1963.

---

[1]Vice President, AICO co. ltd.

[2]Professor, Dept. of Urban and Environmental Engineering, Aichi Institute of Technology

[3]Director, [4]Manager, [5]Assistant Manager, Taisei Rotec co., ltd